

- PENFIELD, K. W., GEWIRTH, A. A. & SOLOMON, E. I. (1985). *J. Am. Chem. Soc.* **107**, 4519–4529.
- PETRATOS, K. (1984). PhD Thesis, Wayne State Univ., Detroit, USA.
- PETRATOS, K., BANNER, D. W., BEPPU, T., WILSON, K. S. & TSERNOGLOU, D. (1987). *FEBS Lett.* **218**, 209–214.
- RAMAKRISHNAN, C. & RAMACHANDRAN, G. N. (1965). *Biophys. J.* **5**, 909–933.
- ROSSMANN, M. G. (1979). *J. Appl. Cryst.* **12**, 225–238.
- WATENPAUGH, K. D., SIEKER, L. C., HERRIOTT, J. R. & JENSEN, L. H. (1973). *Acta Cryst.* **B29**, 943–956.
- WILSON, A. J. C. (1949). *Acta Cryst.* **2**, 318–321.

Acta Cryst. (1988). **B44**, 636–645

Charge-Density Study of Boron Nitrilotriacetate, $C_6H_6BNO_6$, at 100 K: a Comparison of Polar Bonds

BY P. MOECKLI AND D. SCHWARZENBACH

Institut de Cristallographie, University of Lausanne, BSP Dorigny, CH-1015 Lausanne, Switzerland

H.-B. BÜRGI AND J. HAUSER

Laboratorium für chemische Kristallographie, University of Bern, Freiestrasse 3, CH-3012 Bern, Switzerland

AND B. DELLEY

Paul Scherrer Institut für Nuklearforschung, RCA Laboratory, Badenerstrasse 569, CH-8048 Zürich, Switzerland

(Received 1 December 1987; accepted 3 June 1988)

Abstract

The charge density in the cage molecule boron nitrilotriacetate has been determined experimentally at 100 K from X-ray (Mo $K\alpha$, $\lambda = 0.71069$ Å) diffraction data measured to $(\sin\theta/\lambda)_{\max} = 1.08$ Å⁻¹, and calculated theoretically using an efficient and accurate density functional approach. The structure is non-centrosymmetric, orthorhombic space group $Pn2_1a$, $a = 10.468$ (2), $b = 10.193$ (7), $c = 6.754$ (3) Å, $Z = 4$. The electron density has been refined by least squares to $R_F = 0.77\%$. The model includes aspherical rigid atoms represented by a multipole expansion truncated at the hexadecapole level, spherical H atoms, isotropic secondary extinction and the standard structural parameters. Monopolar radial functions were either exponential functions, or free-atom valence-shell functions modified by the κ formalism. The deformation density was constrained to the noncrystallographic molecular symmetry $3m$; partially relaxing this symmetry did not reveal features attributable to intermolecular interactions. Static and dynamic maps with infinite and finite resolutions are presented for both types of monopolar radial functions. The theoretical charge density is in good agreement with the observations. Charge densities in the six bonding regions C–C, B–N, C–N, B–O, C–O and C=O are discussed in terms of peak height and bond polarity: the more electron rich the atoms are, the lower are the peaks; bond peaks tend to be displaced towards the more

electronegative atom. In contradiction with chemical expectation, B–N appears to be more polar than B–O, and C–N more polar than C–O. This is due to the representation of the bonding density as $\rho(\text{observed}) - \rho(\text{promolecule})$.

Introduction

Fig. 1 shows a plot of boron nitrilotriacetate, $C_6H_6BNO_6$ (NTA-B), and the numbering of the atoms. An earlier determination of the crystal and molecular structure of this compound (Müller & Bürgi, 1984) suggested a number of reasons for studying details of the charge-density distribution. Some of these are of a chemical, others of a methodological nature.*

Chemically, NTA-B shows six different types of bonds between B, C, N and O atoms. This fact allows

* For the terminology used in this paper see Coppens (1982).

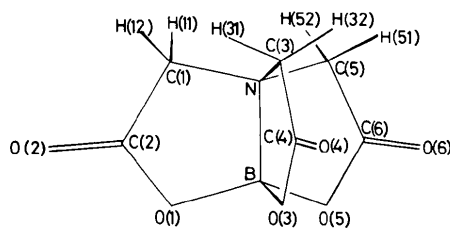


Fig. 1. Numbering of the atoms of the NTA-B molecule.

several comparisons to be made: (1) There are two pairs of what one might call *isoelectronic* bonds, namely B–N and C–C, as well as B–O and C–N; the bonds of each pair differ in polarity but are isoelectronic in the sense that formally the number of electrons contributed by the two spherically symmetric atoms of the promolecule to the bonding region is the same, namely 2 and 2.25 electrons respectively. (2) Both B and C form different types of bonds with atoms of different electronegativity; the bonds B–N, B–O, as well as C–C, C–N, C–O, are increasingly polar and involve an increasing number of electrons in the bonding region. (3) Finally, there are two different types of C–O bonds, a C–O double bond of length 1.206 Å and a C–O ester bond of length 1.334 Å. These facts make it possible to study the influence of electronegativity difference, number of valence electrons and bond length on the appearance of bonding electron density in polar bonds. The comparison between different bonds should be optimal in the sense that the effects of systematic errors in the data, including the deficiencies of the electron-density model, should be similar for all atoms and bond types. This is in contrast to comparisons between different compounds for which errors of at least two experiments accumulate.

On the methodological side, one may note the following: (1) The values of the displacement parameters are relatively low. At 100 K, eigenvalues of the U tensors are in the range of 0.005 to 0.020 Å² for the peripheral carbonyl O atoms, and 0.005 to 0.012 Å² for the atoms in the tricyclic molecular framework. (2) The space group of NTA-B is noncentrosymmetric, and the phases of the structure factors are only incompletely determined by the procrystal structure. Because of this indetermination, several slightly different electron-density models may differ essentially in the phases of the structure factors and reproduce the observations equally well (see below). The additional flexibility in the least-squares fitting of a model may be expected to produce deceptively low reliability indices. A demonstration of the feasibility of a charge-density study with X-ray data alone is in this case of particular interest. The careful study of urea by Swaminathan, Craven, Spackman & Stewart (1984) provides interesting evidence concerning this problem. These authors demonstrate the successful application of a deformation model to a noncentrosymmetric electron-density distribution; in their refinement with respect to the X-ray data, the positional and displacement parameters, as well as a scale factor and the radial exponents of the deformation functions, were kept invariant with numerical values obtained from independent sources. In the present work on NTA-B, all these parameters are part of the refined model. (3) The crystal structure of NTA-B has the approximate molecular symmetry *3m*. The flexibility of the model and the danger of obtaining physically doubtful results may be reduced by making

use of this noncrystallographic symmetry. (4) The molecule of NTA-B is sufficiently small for carrying out theoretical calculations and subsequent comparisons between theoretical and experimental difference density features.

Experimental

Colourless crystals of C₆H₆BNO₆ with nearly isometric linear dimensions of approximately 0.3 mm were obtained as described by Müller & Bürgi (1984). They are orthorhombic, space group *Pn2₁a* (*C*_{2v}², No. 33, standard setting **a**, **-c**, **b**), *a* = 10.468 (2), *b* = 10.193 (7), *c* = 6.754 (3) Å at 100 K, *Z* = 4. Lattice parameters from 14 reflections (18 < θ < 21°). Intensity measurements at 100 K were made with an Enraf–Nonius CAD-4 diffractometer using graphite-monochromated Mo *K*α radiation (λ = 0.71069 Å), a nitrogen-gas-flow cooling device and the ω -scan technique. The scan angle was (0.7 + 0.35 tanθ)°, the experimentally determined counter aperture widths were 1.32° vertical and 1.75° × tanθ (but not less than 0.43°) horizontal. The following intensities were measured: up to sinθ/λ = 0.3642 Å⁻¹, all symmetry equivalent reflections $\pm h$, $\pm k$, $\pm l$ with a maximum scan time of 10 min and a maximum scan speed of 4° min⁻¹, resulting in a precision $\sigma(I)/I$ of better than 0.02 for almost all reflections; up to sinθ/λ = 0.4813 Å⁻¹, all $\pm h$, $\pm k$, $\pm l$ with the same conditions as above; up to sinθ/λ = 1.08 Å⁻¹, only those $\pm h$, $\pm k$, $\pm l$ which could be measured with a precision better than 0.02 using a maximum scan time of 10 min, and all weaker reflections measurable with a precision between 0.02 and 0.04 in less than 10 min. The indices of the reflections likely to conform to these conditions were calculated with the program *FCGEN* (Ngo Thong & Schwarzenbach, 1983) using the structural parameters obtained from the data up to sinθ/λ = 0.48 Å⁻¹. Five intensity control reflections with widely different intensities and Bragg angles were measured every 7 h. Backgrounds were assessed with the conventional CAD-4 procedure, *i.e.* they were assumed to be the first- and last-sixths of the total scan. The variance of an intensity was computed according to $\sigma^2(I) = \sigma^2(\text{counting statistics}) + (KI)^2$ where *K* ≈ 0.015 was obtained from this formula by analyzing the fluctuations of the control reflections about their mean values. For the variance of the unweighted mean value $\langle I \rangle$ of a set of *n* equivalent intensities *I_i*, the larger of the two quantities $\sigma_1^2(\langle I \rangle) = \sum \sigma^2(I_i)/n^2$ and $\sigma_2^2(\langle I \rangle) = \sum (I_i - \langle I \rangle)^2/n(n-1)$ was chosen. Averaging was carried out in the Laue group *mmm*, *i.e.* Friedel pairs were averaged (see below for structure refinement including Friedel pairs). The 6918 measurements resulted in 1711 unique intensities. (The number of all unique reflections to sinθ/λ = 1.08 Å⁻¹ including the ones not measured is about 3800). Eight of these had $\langle I \rangle < 3\sigma(\langle I \rangle)$. The

internal R value was 0.009. The ratio of the largest and smallest intensities is 3300:1, the smallest high-order structure factors are of the order of 6 e (e.s.d. = 0.1 e, $F(000) = 408$ e). The linear absorption coefficient is 0.1528 mm⁻¹. The corresponding absorption factors and mean-path lengths for a sphere of radius 0.15 mm are 1.036 and 0.0255 mm and nearly constant at all Bragg angles (Flack & Vincent, 1978).

Charge-density refinements

All refinements were full matrix and with respect to $|F_o|^2$. The free-atom core and valence-shell scattering factors for C, B, N and O were taken from Fukamachi (1971); the scattering factor for spherically bonded H and the dispersion corrections were from *International Tables for X-ray Crystallography* (1974). The origin along the polar direction was fixed by constraining the sum of the y coordinates of all non-H atoms according to $y(\text{B}) = \text{constant} - \sum y(\text{C,N,O})$. Refinements were terminated when changes in the goodness of fit were smaller than 10^{-4} and all shifts were well below 0.1 e.s.d.'s.

The initial refinement (I) of the standard parameters, *i.e.* scale, isotropic extinction, enantiomorph-polarity (Flack, 1983), positional and thermal parameters, was carried out with a locally improved version of *CRYLSQ* of the *XRAY* system (Stewart, Kruger, Ammon, Dickinson & Hall, 1972). The refinement of the enantiomorph-polarity parameter was carried out on a data set obtained by averaging equivalent intensities according to the point group $m2m$, and therefore containing Friedel pairs h, k, l and $-h, -k, -l$. It converged very fast to 0.0 with an e.s.d. of 0.4, independently of the starting value. This indicates that the crystal used for the measurements was probably a single crystal. However, the large e.s.d. justifies averaging of the Friedel pairs for the subsequent charge-density refinements. These were carried out with the program *LSEXP* (Restori & Schwarzenbach, 1986). The following options were used:*

(a) An isotropic type I extinction correction with Lorentzian mosaic distribution (Becker & Coppens, 1974) was included.

(b) H atoms were refined isotropically but otherwise unconstrained, in order to optimally model with the standard parameters the total electron density in the C-H bonds in whose features we were not interested. The planes H-C-H are perpendicular to the planes of the five-membered rings studied in this paper.

* Lists of structure factors and positional displacement and deformation parameters of refinements I to IV, and maps not reproduced in this paper have been deposited with the British Library Document Supply Centre as Supplementary Publication No. SUP 51066 (27 pp.). Copies may be obtained through The Executive Secretary, International Union of Crystallography, 5 Abbey Square, Chester CH1 2HU, England.

(c) Aspherical components of the atoms C, B, N and O are represented by a sum of up to 35 multipolar deformation functions

$$\rho_{nlm\pm} = P_{nlm\pm} \rho_n(r) C_{lm\pm} y_{lm\pm}, \quad \rho_n(r) = K_n r^n \exp(-ar) \quad (1)$$

(Stewart, 1976) which are exactly equivalent through a linear transformation to the deformation functions of Hirshfeld (1977). Refinable variables are the population factors $P_{nlm\pm}$, and the radial exponents α . The $y_{lm\pm}$ are spherical surface harmonics and the $C_{lm\pm}$ and K_n are normalization factors.

(d) The molecule of $\text{C}_6\text{H}_6\text{BNO}_6$ possesses to a very good approximation the symmetry $3m$. The five-membered rings are nearly planar with a maximum deviation from the least-squares plane of 0.02 Å; they form angles of 58.4, 60.7 and 60.9°. The flexibility of the model was limited by imposing this symmetry on the deformation density rather than by omitting hexadecapolar functions or including only one dipolar and one quadrupolar radial function. With respect to the deformation density parameters, the independent atoms were therefore B and N with point symmetry $3m$, and C(1), C(2), O(1) and O(2) with symmetry m . The deformation functions of the other atoms were generated by the molecular symmetry (Hirshfeld, 1977). Each of the atoms was assigned two sets of dipolar ($n = 1, 3$), two sets of quadrupolar ($n = 2, 4$), and one set each of octopolar ($n = 3$) and hexadecapolar ($n = 4$) functions. Positional and displacement parameters were refined independently for all 20 atoms.

(e) In refinement II, the monopoles were represented by the κ formalism (Coppens, Guru Row, Leung, Stevens, Becker & Yang, 1979) including an explicit constraint to ensure electroneutrality. In refinement III, they were represented by the two exponential functions with $n = 0$ and 2, and the electroneutrality was imposed with a restraint on $F(000)$. Including one radial exponent α per atom, this results in 109 deformation parameters in II, and 110 in III.

(f) Each of the keto O atoms O(2), O(4) and O(6) has two relatively short contact distances to carboxyl C atoms C(2), C(4) and/or C(6) of neighbouring molecules, ranging from 2.926 to 3.049 (2) Å. These were interpreted by Müller & Bürgi (1984) as intermolecular interactions. They do not conform to the molecular symmetry $3m$. Therefore, in a subsequent refinement (IV) with κ -type monopoles, the keto O atoms were treated as independent atoms with point symmetry 1, while the rest of the molecule remained constrained to a symmetry $3m$. The number of refined deformation parameters was thereby increased by 83 to 192.

The following deformation density maps were calculated including all the multipolar deformation functions described above:

(a) Dynamic doubly phased $X' - X$ Fourier maps at experimental resolution, using Fourier coefficients $[F_o$

(phases of refinements II, III or IV) – F_c (spherical atom model with parameters of refinements II, III or IV)], $(\sin\theta/\lambda)_{\max} = 1.08 \text{ \AA}^{-1}$.

(b) Static Fourier maps (multipole deformation maps) at experimental resolution, using Fourier coefficients computed with the deformation parameters of refinements II, III or IV, $(\sin\theta/\lambda)_{\max} = 1.08 \text{ \AA}^{-1}$.

(c) Static model maps (multipole deformation maps) at infinite resolution obtained by summing the deformation functions of refinement III in direct space. All neighbouring atoms within 3 Å of the molecule were included. The e.s.d. of this deformation density was computed using the variance-covariance matrix obtained in the refinement (Hirshfeld, 1977).

Differences between refinements

Some characteristic results obtained from refinements I to IV are shown in Table 1. The reliability indices are greatly improved in going from the spherical-atom model to the charge-density models. Those of models II and III are very similar. The corresponding scale factors differ, however, by 2.3%. This considerable spread of values reflects the uncertainty (inaccuracy) inherent in the choice of a model for the deformation density, whereas the e.s.d.'s and the goodness of fit indicate the much superior precision of the fit of a particular model to the observations. Convergence in II and IV was considerably faster than in III where correlation coefficients between scale, anisotropic displacement and monopolar population parameters were larger, reaching values of about 0.9. This numerical stability of the κ formalism represents an, at least technical, advantage over the exponential functions. The radial exponents α of C(1,3,5), C(2,4,6), B, N, O(1,3,5) and O(2,4,6) converged respectively to 5.2 (2), 4.6 (1), 3.9 (2), 6.0 (3), 8.1 (7) and 3.2 (1) Å⁻¹ in II, and to 5.3 (2), 4.6 (1), 4.0 (2), 6.5 (4), 7.9 (6) and 3.6 (1) Å⁻¹ in III. All these values are smaller than the standard ones recommended by Hehre, Stewart & Pople (1969), the most notable difference occurring for the very diffuse double-bonded O(2,4,6). The differences between models are also evident from the anisotropic displacement parameters. The diagonal elements of the U tensors are systematically larger in III than in II: the differences are 0.00006 to 0.00010 Å² for B, and 0.0002 to 0.0003 Å² for C, N and O, with e.s.d.'s of 0.000016 Å².

Lowest reliability indices were obtained in refinement IV. However, as discussed below, the blurred features observed on the corresponding deformation maps in the region of the keto O atoms are less credible than those of the much cleaner maps obtained with the more restricted refinements II and III. It may well be that the data set is not sufficiently accurate for refining this more flexible model, although there were no numerical problems of convergence.

Table 1. Reliability and scale factors

I: standard spherical-atom refinement; II: deformation density with κ monopoles, symmetry $3m$; III: deformation density with monopoles represented by exponential functions, symmetry $3m$; IV: deformation density with κ monopoles, O(2), O(4) and O(6) refined independently with symmetry 1.

	I	II	III	IV
Goodness of fit				
$S(F ^2) \approx S(F)$	4.4945	1.3768	1.3785	1.2902
$R(F)$ for all reflections	0.0223	0.00770	0.00773	0.00696
$wR(F ^2) \approx 2wR(F)$	0.0588	0.01716	0.01718	0.01562
No. of variables	150	260	261	343
Scale factor $F_c = \text{scale} \times F_c$	4.732 (6)	4.684 (8)	4.794 (19)	4.668 (8)

The extinction parameter in the standard refinement I converged to negative values and was reset to zero. In all deformation refinements II, III and IV, however, the extinction correction is *not* negligible. It is very similar in II and III, and slightly less important in IV: the smallest extinction factors y_{\min} ($F_c = yF_{\text{corr}}$) obtained in these refinements are 0.9040, 0.9036 and 0.9430, respectively. In II and III, there are two additional y values between 0.96 and 0.97, three between 0.97 and 0.98, and 14 between 0.98 and 0.99. In IV, there are altogether only eight reflections with y smaller than 0.99. This clearly shows the danger of accepting an extinction correction obtained from a standard spherical-atom refinement, or maybe of accepting the result of any extinction refinement at face value.

Results

Standard parameters

Positional and displacement parameters of II and III agree closely. In comparison with I, the bond lengths agree somewhat better with the molecular symmetry $3m$, but the deviations from, and angles between, the least-squares planes hardly change. The largest changes occur for the C–H distances which vary from 0.909 to 0.972 (20) Å in I, but only from 0.955 to 0.973 (20) Å in III. Mean bond lengths obtained in III are 1.5179 (8), 1.6273 (8), 1.4989 (9), 1.4477 (10), 1.3339 (9) and 1.2058 (7) Å for C–C, B–N, C–N, B–O, C–O and C=O, respectively.

The displacement parameters were analyzed with respect to the rigid-bond criterion (Hirshfeld, 1976), and the rigid-body TLS model (Schomaker & Trueblood, 1968). The rigid-bond criterion states that the difference $|\Delta z^2|$ of the mean-square displacements of two atoms along a covalent bond should be small. All bonds of a rigid-body molecule are rigid. The standard refinement I resulted in $|\Delta z^2|$ values ranging from 0.0000 to 0.0018 (3) Å² for which no correlation with the molecular symmetry could be detected. In the deformation refinements, the $|\Delta z^2|$ values are significantly smaller. They range from 0.0000 to 0.0009 (2) Å² in II, and from 0.0000 to 0.0007 (2) Å² in III. In both cases, values for the least-rigid bonds

Table 2. *Eigenvalues of the L (rad²) and T (Å²) tensors for refinements I to III*

Model III' includes a torsional vibration about the B–N bond with a mean-square amplitude $\langle\omega^2\rangle + 2c\langle\omega^2\rangle^{1/2}L_{1,1/2}$ of 0.00096 (9) rad².

	I	II	III	III'
L_1	0.00102	0.00106	0.00107	0.00106
L_2	0.00087	0.00088	0.00088	0.00086
L_3	0.00079	0.00079	0.00079	0.00077
E.s.d.	0.00010	0.00007	0.00007	0.00005
T_1	0.00644	0.00606	0.00627	0.00565
T_2	0.00584	0.00549	0.00568	0.00522
T_3	0.00527	0.00509	0.00528	0.00503
E.s.d.	0.00030	0.00020	0.00020	0.00013
ωR	0.113	0.078	0.078	0.044

$\Delta z^2(\text{N–B})$, $\Delta z^2(\text{O–B})$, and to a lesser degree also for $\Delta z^2(\text{N–C})$, are negative. This indicates that vibrational displacements are larger for the lighter atoms B and C, and smaller for the heavier atoms N and O, in agreement with general expectations from the theory of normal vibrations.

The agreement of the refined U tensors with those calculated from the TLS model (Table 2) improved in going from the spherical-atom model to the deformation models. The weighted reliability index $R = \sum w(U_{ij}^{\text{obs}} - U_{ij}^{\text{calc}})^2 / \sum w(U_{ij}^{\text{obs}})^2$ is 0.113 for refinement I, but 0.078 for II and III. The eigenvalues of L are very similar for models I, II and III. Those of T show changes at the limit of significance; however, they are the same for all values T_i and thus systematic. This indicates that differences ΔU_{ij} which determine L are more reliable than absolute magnitudes U_{ij} which

determine T. The latter depend on the electron-density model (as does the scale factor) and on the quality of the data (Chandrasekhar & Bürgi, 1984).

The analysis of the U_{ij}^{obs} was carried a step further. The main discrepancies $U_{ij}^{\text{obs}} - U_{ij}^{\text{calc}}$ in II and III are found for the atoms C(1), C(3), C(5) and O(1), O(3), O(5) in directions perpendicular to the five-membered rings; they are all significant and positive. They may be interpreted in terms of a low-frequency torsional vibration about the B–N bond with symmetry A_2 in which the motion of C(1), C(3), C(5) is correlated and opposite in direction to that of O(1), O(3), O(5). The softness of this mode is plausible in view of the equilibrium structure of the cage molecule in which the B–N, N–C and B–O bonds are all stereochemically constrained into the energetically unfavourable eclipsed conformation. Torsional oscillation about B–N deforms all these conformational angles towards an energetically more favourable staggered arrangement, albeit at the expense of making the B–O(1,3,5)–C(2,4,6)=O(2,4,6) and N–C(1,3,5)–C(2,4,6)=O(2,4,6) fragments nonplanar. Including this motion in the analysis of U^{obs} adds six extra parameters to the TLS analysis (Dunitz, Schomaker & Trueblood, 1988). By far the most important of them involves the mean-square amplitude $\langle\omega^2\rangle$ of the internal rotation about B–N; more precisely, the most important parameter is the sum $\bar{\omega} = \langle\omega^2\rangle + 2c\langle\omega^2\rangle^{1/2}L_{1,1/2}$, where $L_{1,1} \approx L_1$ is the molecular libration about the direction of the B–N bond, and c expresses the correlation between $\langle\omega^2\rangle$ and $L_{1,1}$. The fit between U_{ij}^{obs} and U_{ij}^{calc} obtained with this model is substantially better (Table 2, model III'). The value of 0.00096 (9) rad² obtained for $\bar{\omega}$ is of almost the same magnitude as L_1 .

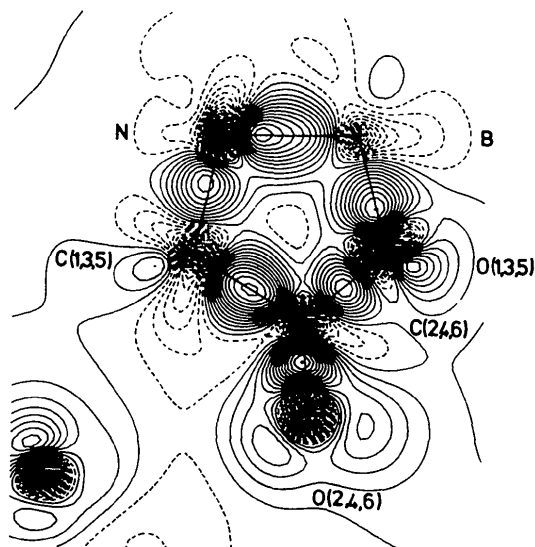


Fig. 2. Static model map at infinite resolution through the least-squares plane of a chelate ring, refinement III. Interval 0.05 e Å⁻³, negative contours broken. E.s.d.'s calculated from the inverse of the normal-equations matrix are 0.02 e Å⁻³ between the atoms, and increase to 0.6, 0.4, 0.18, 0.16, 0.12 and 0.12 e Å⁻³ at the sites of O(1,3,5), N, C(1,3,5), O(2,4,6), C(2,4,6) and B, respectively.

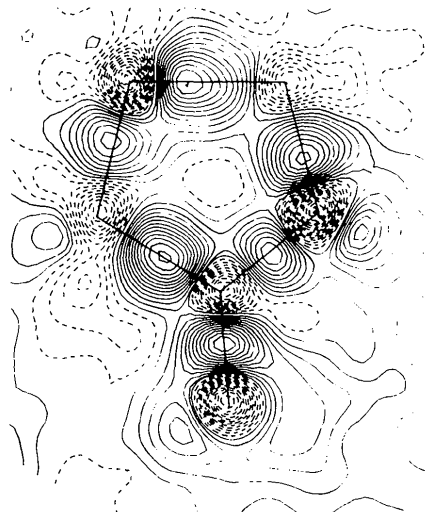
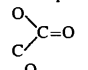


Fig. 3. Static Fourier map at experimental resolution, through the chelate ring B–N–C(1)–C(2), O(2)–O(1), refinement III. Intervals and identification of the atoms as for Fig. 2. The other chelate rings are identical.

Table 3. *Bonding and lone-pair difference densities*

Peak heights $\Delta\rho_{\max}$ ($e \text{ \AA}^{-3}$), e.s.d.'s as computed from the inverse of the matrix of the normal equations are $0.02 e \text{ \AA}^{-3}$; Asym., the distance of the bonding maximum from the midpoint of the bond in percent of the bond length, a positive value indicating that the peak on the bond $X-Y$ is displaced towards Y . Refinements I, II and III are defined in the text.

Bond $X-Y$	Theoretical		Exponential, III		Exponential, III		κ Monopoles, II			Procrystal, I	
	Asym.	$\Delta\rho_{\max}$	Infinite resolution Asym.	$\Delta\rho_{\max}$	Asym.	Static $\Delta\rho_{\max}$	$X'-X$ $\Delta\rho_{\max}$	Asym.	Static $\Delta\rho_{\max}$	$X'-X$ $\Delta\rho_{\max}$	$X-X$ $\Delta\rho_{\max}$
C=O	-10	0.70	-10	0.70	-5	0.55	0.50	-8	0.60	0.55	0.25
C-C(O ₂)	-1	0.50	2	0.60	5	0.60	0.50	2	0.60	0.55	0.25
B-N	38	0.85	21	0.55	13	0.55	0.50	15	0.55	0.50	0.30
B-O	12	0.40	12	0.55	8	0.50	0.45	7	0.55	0.50	0.30
C-N	6	0.35	7	0.40	5	0.35	0.30	5	0.35	0.30	0.15
C-O	1	0.40	-1	0.40	0	0.35	0.35	0	0.45	0.35	0.25
Lone pairs											
	}	>1.00	0.20	0.15	0.20	0.20	0.20	0.20	0.20	0.20	0.20
		>1.00	0.15	0.20	0.15	0.20	0.20	0.20	0.15	0.15	
-O-		>1.00	0.35	0.30	0.30	0.45	0.35	0.20			

Standard parameters from refinement IV are in close agreement with those from II and III. An in-depth discussion of them appears to be unnecessary, since model IV represents no improvement over models II and III (see below). In summary, we note that the standard parameters are chemically and physically more reasonable for the complete electron-density models than they are for the standard spherical-atom model.

Deformation density maps

Figs. 2-5 show some of the deformation density maps obtained with refinements II and III. Table 3 lists the peak heights of the observed bonding and lone-pair densities, and the displacements of the bond peaks from the midpoints of the bonds.

An $X-X$ difference density map (not shown here) computed after standard refinement I shows diffuse

features, including low bonding maxima near the midpoints of all bonds and lone-pair maxima near all O atoms. The maps resulting from II and III differ qualitatively from that obtained with I: the bond peaks are now twice as high, and they tend to be displaced from the midpoints of the bonds toward the more electronegative atom. Overall, Table 3 shows satisfactory agreement between II and III.

The differences in peak heights between infinite and finite resolution (Figs. 2, 3), or between static and dynamic maps (Figs. 3, 4) follow expected trends, but are relatively minor. Fourier maps at finite resolution (Figs. 3, 4, 5) were computed including only those Fourier terms corresponding to measured structure factors. *A priori*, the contribution of the unmeasured high-order structure factors cannot be assumed to be small; but comparison with Fig. 2 shows that this contribution is indeed negligible. The features of the maps corresponding to II and III (Figs. 3, 5) differ at

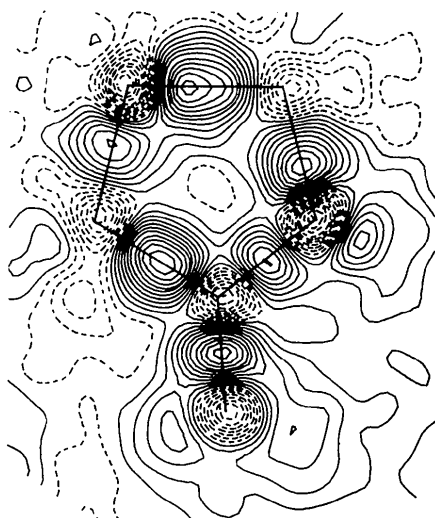


Fig. 4. Dynamic doubly phased $X' - X$ Fourier map, refinement III, atoms and intervals as in Figs. 2 and 3. The other chelate rings are very similar.

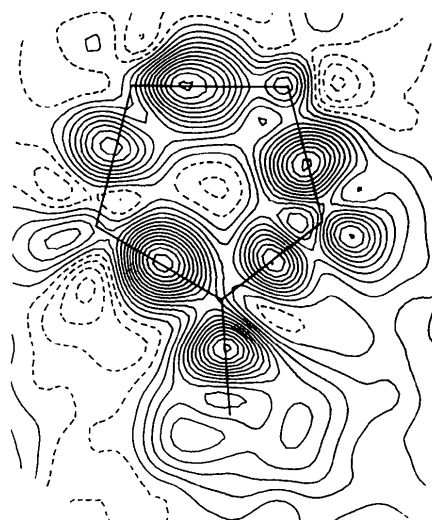


Fig. 5. Static Fourier map at experimental resolution, analogous to Fig. 3, refinement II.

the atomic centres by much more than allowed on the basis of their standard deviations. It is there that the difference of the respective scale factors shows its greatest effect: the κ monopoles do not produce any holes, in contrast to the exponential functions.

Sections of the electron-density function perpendicular to the chelate ring, e.g. through the lone-pair densities of O(2,4,6) and O(1,3,5), and through the midpoints of the bonds, present no unexpected features and no densities elongated perpendicular to the mirror plane. For this reason, they are given only as Supplementary Material.* The low maximum in the chelate ring plane near C(1,3,5) is due to low residual densities of $0.25 \text{ e } \text{Å}^{-3}$ (infinite resolution) situated on the C—H bonds. These have no physical significance because of the unsophisticated treatment of the H atoms. The deformation maps resulting from refinement IV where the symmetry $3m$ was relaxed for the keto O atoms, are included in the Supplementary Material.* Difference densities near O(2), O(4), and to a lesser degree O(6), are still approximately symmetric with respect to the chelate ring, the lone-pair features still peak in the plane of the chelate ring, and there are no indications of interactions with carboxyl C atoms of neighbouring molecules. General features and bond peak asymmetries agree with Figs. 2 to 5. However, the two lone-pair peaks of O(2,4,6) are now asymmetric and ill resolved, in particular for O(2) and O(6). In addition, some of the bond peak heights have changed by more than three e.s.d.'s. We believe that this charge-density model is too flexible and also parametrizes part of the systematic errors of the data. The absence in IV of features attributable to intermolecular interactions, and of notable deviations from the molecular symmetry $3m$, justifies the adoption of the $3m$ symmetry constraint of refinements II and III and the acceptance of Figs. 2 to 5 as more trustworthy results.

Residual maps were computed with Fourier coefficients [$F_o - F_c$ (models II, III)] and the phases of the respective models. They show mainly the zero contour lines and no recognizable features. Maximum densities are $0.05 \text{ e } \text{Å}^{-3}$. E.s.d.'s at the atomic sites are surprisingly low (caption of Fig. 2). This may be due to the lack of a centre of symmetry which permits more flexible modeling even in regions close to the atomic nuclei where the diffraction data carry little information. A similar effect has been observed for the noncentrosymmetric structure of AlPO_4 (Ngo Thong & Schwarzenbach, 1979).

Theoretical calculations

Theoretical calculations were based on the density functional approach (Hohenberg & Kohn, 1964; Kohn

& Sham, 1965). The density is constructed from N single-particle orbitals Φ_i occupied according to the Fermi distribution at zero temperature:

$$\rho(\mathbf{r}) = 2 \sum_i |\Phi_i(\mathbf{r})|^2. \quad (2)$$

The single-particle functions obey self-consistent equations

$$\{-(\hbar^2/2m)\Delta + V_{\text{electrostatic}}(\mathbf{r}) + \mu_{\text{xc}}[\rho(\mathbf{r})]\}\Phi_i(\mathbf{r}) = \varepsilon_i \Phi_i(\mathbf{r}), \quad (3)$$

where $V_{\text{electrostatic}}$ is the potential due to the nuclei and the electrons, and exchange and correlation are taken into account by the effective potential μ_{xc} according to Hedin & Lundqvist (1971). Equation (3) is solved by a Ritz variation method. The functions Φ_i are expanded in a basis set consisting of atomic functions taken from a numerical difference equation solution of (3) for spherical atoms, plus the corresponding functions for ions, and in addition a double set of tight polarization functions s , p , d for the non-H atoms and s , p for H. This basis set permits proper dissociation into density functional atoms, the dissociation limit being attained exactly. More than 98% of the molecular binding energy corresponding to the exact local-density functional is thereby obtained. Integrations for the matrix elements in the secular equation were performed numerically using a single set of integration points and weights in order to take advantage of the discrete variational scheme of Ellis & Painter (1970). For the calculation of the potential $V_{\text{electrostatic}}$, $\rho(\mathbf{r})$ is expanded into a flexible charge basis set (Delley & Ellis, 1982) truncated at quadrupoles for the non-H atoms and at dipoles for H. For this method, the computational effort grows only with the third power of the size of the molecule. The coordinates used for the non-H atoms were obtained by imposing the molecular symmetry $3m$ on the crystallographic coordinates. H positions were calculated for a C—H bond length of 1.08 Å . The calculated deformation density shown in Fig. 6 was obtained by subtracting from the total charge density a promolecule density built up from spherical density functional atoms.

Based on the experience gained with extensive tests of the method on small molecules, the deformation density near midbond is assumed to be within $\{+0, -0.1\} \text{ e } \text{Å}^{-3}$ of a hypothetical exact local-density functional $\rho(\mathbf{r})$. Excellent basis flexibility is suggested by the small electric fields at the nuclei which should ideally be zero according to the Hellmann–Feynman theorem: absolute values at non-H-atom positions range from 0.003 to 0.01 a.u. (0.15 to 0.51 MV m^{-1}). With the Hartree–Fock method, comparably small fields have been obtained only for diatomic molecules. Deviations from zero field are due to basis-set incompleteness, and also to the fact that the atomic positions used for the calculations do not coincide exactly with the equilibrium positions of the density functional. The

* See deposition footnote.

calculated dipole moment of NTA-B is 7.5 debye (25×10^{-30} C m) with the positive charge on N. The calculated quadrupole moment is 67 Buckingham (223.5×10^{-40} C m²). Calculations were carried out with a VAX-780 computer; the time necessary to reach self consistency was 546 min.

Discussion

The theoretical results (Fig. 6) are to be compared with the experimental static map at infinite resolution (Fig. 2). The maps show generally good agreement in the bonding regions which attests the high quality of the density functional approach, and the appropriateness of the electron-density refinement methods for this non-centrosymmetric structure. Significant differences occur, however, within about 0.2 to 0.3 Å of the atoms. There, the theoretical calculation shows sharp features which are not present in the experimental density. Consider, for example, the C—C and B—N bonds of Fig. 6: C—C shows difference density peaks at 0.25 Å from the C atoms and at the midpoint of the bond; B—N shows a small peak close to B and a sharp maximum peaking at 0.2 Å from N which extends well beyond the midpoint of the bond. Analogous, but less-pronounced features are found for the other isoelectronic pair of bonds, C—N and B—O. The model for the deformation density fitted to the limited amount of diffraction data available renders only a blurred image of these features. It indicates that of all of the bonds, B—N is the most asymmetric, but the bond peak is not displaced far enough towards N and it is not high enough (Table 3). This is explained by the fact that the experimental information on regions close to atomic sites is weak. There, the experimental density is

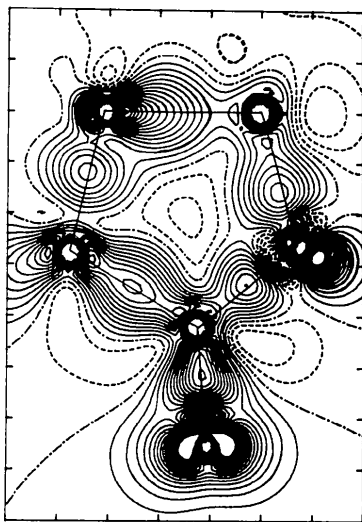


Fig. 6. Theoretical deformation map. Identification of the atoms and intervals as in Fig. 2.

imprecise (large e.s.d.) as well as inaccurate (due to deficiencies of the model, *inter alia* manifested by the uncertainty in the scale factor), since the resolving power of the diffraction data is only of the order of 0.5 Å. Features on a much smaller scale are introduced by the model rather than the experiment.

The lone-pair features near O show similar discrepancies which may again be rationalized by the lack of resolution of the data. On the theoretical map, the maxima are very sharp and at distances of only 0.2 Å from the atomic centres. On the experimental map, they are rather diffuse, particularly those peaking at about 0.6 Å from O(2,4,6), in agreement with the corresponding value of only 3.6 (1) Å⁻¹ for the radial exponent α of the deformation functions. This may be due to incomplete deconvolution of thermal motion and/or to biased positional coordinates, which are indeed most likely to occur for the keto O(2,4,6) atoms. Similar low features have been obtained for X—X and X—N maps, as e.g. in diformohydrazide (Eisenstein, 1979), C₆H₁₂N₄O₄ (Dunitz & Seiler, 1983), and oxalic acid dihydrate (Commission on Charge, Spin and Momentum Densities, 1984). In contrast, model maps computed with a large value of $\alpha(O)$, either fixed at the theoretical value of 8.5 Å⁻¹ of Hehre, Stewart & Pople (1969) or obtained in the refinement, show lone-pair maxima which are at least as important as the C=O bond maxima and at distances smaller than the experimental resolution, as e.g. in urea (Swaminathan, Craven, Spackman & Stewart, 1984), in parabanic acid (He, Swaminathan, Craven & McMullan, 1988), in the 1:1 complex of thiourea with parabanic acid (Weber & Craven, 1987), near O(4) in 5,5-diethylbarbituric acid (barbital II; Craven, Fox & Weber, 1982) and in diformohydrazide. These relatively sharp maxima may to some extent show properties of the model, and not of the experiment.

Judging from the experimental, and more clearly from the theoretical map, the B—N bond appears to be particularly remarkable: its difference density may be described as intermediate between the lone-pair region of O(1,3,5) and the C—C internuclear region. In view of the rather long B—N distance of 1.627 Å, it is tempting to interpret this in terms of a dative bond between an N lone pair and an empty orbital on B.

The order of the bonds according to the heights of the bonding maxima in Fig. 2 is C=O \approx C—C > B—N \approx B—O > C—N \approx C—O (or B—N taking the first place according to Fig. 6). Excluding the C—O double bond, this sequence is roughly the reverse of that given by the number of valence electrons formally contributed by the bonded atoms to the bonding region: if each atom contributes $\frac{1}{2}$ of its valence electrons, these numbers are 2, 2, 2.25, 2.25 and 2.5, respectively. An increasing deficit of difference electron density in the region between electron-rich atoms has also been described by Dunitz & Seiler (1983). These authors find

about $0.35 \text{ e } \text{Å}^{-3}$ for C–N, 0.3 and $0.25 \text{ e } \text{Å}^{-3}$ for C–O and N–N, and a negative value for O–O. The same order of C–C and C–N peak heights has also been found in barbital (Craven, Fox & Weber, 1982); in parabanic acid (Weber & Craven, 1987; He, Swaminathan, Craven & McMullan, 1988), the heights of the C–C and C–N peaks are very similar; and in urea (Swaminathan, Craven, Spackman & Stewart, 1984), the C–N peaks are as high as, or higher than the C=O maxima. In the last three compounds, the C–N bond lengths are considerably shorter (1.35 to 1.39 Å) than in NTA-B (1.50 Å) and the corresponding bond peaks are therefore higher (0.45 to $0.70 \text{ e } \text{Å}^{-3}$), whereas C–C bond lengths and bond peaks are similar in all the compounds.

The order of the bonds according to the asymmetry of the bonding density is $\text{B–N} > \text{B–O} \approx \text{C=O} > \text{C–N} > \text{C–C} \approx \text{C–O}$. The maxima tend to be displaced towards the more electronegative atom, except in C=O. Analogous effects are observed in the electron densities mentioned above, except in barbital and in one of the studies of parabanic acid (Weber & Craven, 1987) where the C–N bonds are polarized towards C. One might ask why the order in asymmetry is clearly $\text{B–N} > \text{B–O}$ and $\text{C–N} > \text{C–O}$, rather than the reverse as expected from the corresponding electronegativities; or why C=O is polarized towards C. The effect may be attributed to the representation of the charge density as difference density $\Delta\rho = \rho(\text{observed}) - \rho(\text{promolecule})$ where the promolecule consists of *spherically averaged* free atoms. The B–O bond appears to be less polar because more density is subtracted around O than around N. The same argument applies to the other pair of bonds.

Support for this hypothesis comes from simple model calculations using p orbitals ϕ_X and ϕ_Y centered on atoms X and Y and oriented along $X\text{--}Y$. The electron density on the bond is then

$$\rho = 2|c_X\phi_X + c_Y\phi_Y|^2 / (c_X^2 + c_Y^2 + 2c_Xc_Y S_{XY}) \quad (4)$$

and the procrystal density is

$$\rho_P = n_X\phi_X^2 + n_Y\phi_Y^2, \quad (5)$$

where S_{XY} is the overlap integral and n is taken as one quarter of the number of valence electrons of the atom. Using Slater-type orbitals from Clementi & Raimondi (1963) with exponents and overlap integrals from the tables of Mullikan, Rieke, Orloff & Orloff (1949), we obtain the following characteristics of the difference density $\Delta\rho = \rho - \rho_P$:

(1) In the series C–C, N–N, O–O with bond distances 1.52, 1.44, 1.47 Å, $\Delta\rho_{\text{max}}$ is 0.20, 0.00, $-0.12 \text{ e } \text{Å}^{-3}$, respectively. The calculated trend matches the observed one (Dunitz & Seiler, 1983). We conclude that the model properly reproduces trends.

(2) For $c_X \approx c_Y$, the bonding density is polarized toward the *less* electronegative atom X . For the B–N

and B–O bonds, $\Delta\rho_{\text{max}}$ is 0.19 and $0.20 \text{ e } \text{Å}^{-3}$, and the corresponding asymmetries are -7 and -10% , respectively. Note that the reverse polarization is more pronounced for the more electron-rich (and more electronegative) atom Y .

(3) For $c_X < c_Y$, $\Delta\rho$ is polarized towards Y as expected. However, this polarization is less pronounced if Y is more electron rich. For B–N and B–O with $c_X/c_Y \approx 0.47$, $\Delta\rho_{\text{max}}$ values are 0.25 and $0.15 \text{ e } \text{Å}^{-3}$, and asymmetries are 16 and 5%, respectively.

We conclude, as others have done before (Spackman & Maslen, 1985; Schwarz, Valtazanos & Ruedenberg, 1985; Schwarz, Mensching, Valtazanos & von Niessen, 1986; Kunze & Hall, 1987), that the features appearing in a difference density depend on the type of atomic densities subtracted from the total molecular density. Subtraction of spherically averaged atomic densities brings into prominence the reorganization of atomic charge necessary to prepare the spherical atoms for binding. In the case of N–N and O–O bonds, this choice reduces or eliminates positive features between the atoms (Dunitz & Seiler, 1983); in the case of polar bonds apparently unreasonable polarizations may be simulated. Difference densities obtained by subtracting atoms whose half-filled or empty orbitals are suitably oriented with respect to their environment should highlight charge redistributions accompanying the formation of bonds. The question remains how to define a suitably prepared atom. We cannot answer it and have to pass it on to the theoreticians (for metal–metal bonds, see Hall, 1982, 1986). Until they come up with an answer we have to present our results in terms of the traditional difference density. We end by pointing out once again that our results do *not* imply chemically unreasonable polarization of charge in heteronuclear bonds.

We thank Dr Ngo Thong for help with the measurements and Dr R. Restori for his contributions to the programme LSEXP. The work has been supported by the Swiss National Science Foundation.

References

- BECKER, P. J. & COPPENS, P. (1974). *Acta Cryst.* **A30**, 129–147.
 CHANDRASEKHAR, K. & BÜRGLI, H.-B. (1984). *Acta Cryst.* **B40**, 387–397.
 CLEMENTI, E. & RAIMONDI, D. L. (1963). *J. Chem. Phys.* **38**, 2686–2689.
 COMMISSION ON CHARGE, SPIN AND MOMENTUM DENSITIES (1984). *Acta Cryst.* **A40**, 184–195.
 COPPENS, P. (1982). *Electron Distributions and the Chemical Bond*, edited by P. COPPENS & M. B. HALL, pp. 61–92. New York: Plenum Press.
 COPPENS, P., GURU ROW, T. N., LEUNG, P., STEVENS, E. D., BECKER, P. J. & YANG, Y. W. (1979). *Acta Cryst.* **A35**, 63–72.
 CRAVEN, B. M., FOX, R. O. & WEBER, H.-P. (1982). *Acta Cryst.* **B38**, 1942–1952.
 DELLEY, B. & ELLIS, D. E. (1982). *J. Chem. Phys.* **76**, 1949–1960.

- DUNITZ, J. D., SCHOMAKER, V. & TRUEBLOOD, K. N. (1988). *J. Phys. Chem.* **92**, 856–867.
- DUNITZ, J. D. & SEILER, P. (1983). *J. Am. Chem. Soc.* **105**, 7056–7058.
- EISENSTEIN, M. (1979). *Acta Cryst.* **B35**, 2614–2625.
- ELLIS, D. E. & PAINTER, G. S. (1970). *Phys. Rev. B*, **2**, 2887–2898.
- FLACK, H. D. (1983). *Acta Cryst.* **A39**, 876–881.
- FLACK, H. D. & VINCENT, M. G. (1978). *Acta Cryst.* **A34**, 489–491.
- FUKAMACHI, T. (1971). *Mean X-ray Scattering Factors Calculated from Analytical Roothaan–Hartree–Fock Wave Functions by Clementi*. Tech. Rep. Ser. B, No. 12. Institute for Solid State Physics, Univ. of Tokyo, Japan.
- HALL, M. B. (1982). *Electron Distributions and the Chemical Bond*, edited by P. COPPENS & M. B. HALL, pp. 205–220. New York: Plenum Press.
- HALL, M. B. (1986). *Chem. Scr.* **26**, 389–394.
- HE, X. M., SWAMINATHAN, S., CRAVEN, B. M. & McMULLAN, R. K. (1988). *Acta Cryst.* **B44**, 271–281.
- HEDIN, L. & LUNDQVIST, B. I. (1971). *J. Phys. C*, **4**, 2064–2083.
- HEHRE, W. J., STEWART, R. F. & POPLÉ, J. A. (1969). *J. Chem. Phys.* **51**, 2657–2664.
- HIRSHFELD, F. L. (1976). *Acta Cryst.* **A32**, 239–244.
- HIRSHFELD, F. L. (1977). *Isr. J. Chem.* **16**, 226–229.
- HOHENBERG, P. & KOHN, W. (1964). *Phys. Rev. B*, **136**, 864–871.
- International Tables for X-ray Crystallography* (1974). Vol. IV. Birmingham: Kynoch Press. (Present distributor Kluwer Academic Publishers, Dordrecht.)
- KOHN, W. & SHAM, L. J. (1965). *Phys. Rev. A*, **140**, 1133–1138.
- KUNZE, K. L. & HALL, M. B. (1987). *J. Am. Chem. Soc.* **109**, 7617–7623.
- MÜLLER, E. & BÜRGI, H.-B. (1984). *Helv. Chim. Acta*, **67**, 399–405.
- MULLIKAN, R. S., RIEKE, C. A., ORLOFF, D. & ORLOFF, H. (1949). *J. Chem. Phys.* **17**, 1248–1267.
- NGO THONG & SCHWARZENBACH, D. (1979). *Acta Cryst.* **A35**, 658–664.
- NGO THONG & SCHWARZENBACH, D. (1983). Program *FCGEN* for PDP11/34 computer. Institut de Cristallographie, Univ. of Lausanne, Switzerland.
- RESTORI, R. & SCHWARZENBACH, D. (1986). *Acta Cryst.* **B42**, 201–208.
- SCHOMAKER, V. & TRUEBLOOD, K. N. (1968). *Acta Cryst.* **B24**, 63–76.
- SCHWARZ, W. H. E., MENSCHING, L., VALTAZANOS, P. & VON NIESSEN, W. (1986). *Int. J. Quantum Chem.* **30**, 439–444.
- SCHWARZ, W. H. E., VALTAZANOS, P. & RUEDENBERG, K. (1985). *Theor. Chim. Acta*, **68**, 471–506.
- SPACKMAN, M. A. & MASLEN, E. N. (1985). *Acta Cryst.* **A41**, 347–353.
- STEWART, J. M., KRUGER, G. J., AMMON, H. L., DICKINSON, C. W. & HALL, S. R. (1972). The *XRAY72* system. Tech. Rep. TR-192. Computer Science Center, Univ. of Maryland, College Park, Maryland, USA.
- STEWART, R. F. (1976). *Acta Cryst.* **A32**, 565–574.
- SWAMINATHAN, S., CRAVEN, B. M., SPACKMAN, M. A. & STEWART, R. F. (1984). *Acta Cryst.* **B40**, 398–404.
- WEBER, H.-P. & CRAVEN, B. M. (1987). *Acta Cryst.* **B43**, 202–209.

Acta Cryst. (1988). **B44**, 645–650

Crystal Structure of 2-Bromo-5-hydroxyethoxy-7,7,8,8-tetracyanoquinodimethane, BHTCNQ*

BY R. K. LAIDLAW,† J. BAGHDADCHI,‡ C. A. PANETTA, Y. MIURA§ AND E. TORRES

Department of Chemistry, University of Mississippi, University, MS 38677, USA

AND R. M. METZGER¶

Department of Chemistry, University of Alabama, Tuscaloosa, AL 35487-0336, USA

(Received 31 March 1987; accepted 30 August 1988)

Abstract

2-Bromo-5-(2'-hydroxyethoxy)-7,7,8,8-tetracyanoquinodimethane [*Chemical Abstracts* name: 2-bromo-5-(2'-hydroxyethoxy)-2,2'-(2,5-cyclohexadiene-1,4-

diylidene)bispropanedinitrile, 58268-31-8], $C_{14}H_7BrN_4O_2$, $M_r = 343.14$, monoclinic, $P2_1/n$ (No. 14), $a = 9.258$ (5), $b = 13.618$ (5), $c = 10.947$ (2) Å, $\beta = 92.14$ (4)°, $V = 1379.1$ Å³, $Z = 4$, $D_x = 1.65$ g cm⁻³, $\lambda(Mo K\alpha) = 0.71069$ Å, $\mu = 31.7$ cm⁻¹, $F(000) = 680.0$, $T = 295$ (3) K, $R = 3.9\%$ for 1395 observed reflections. The molecule has an approximate quinoid structure, but there are significant deviations from the *mmm* symmetry of TCNQ; the hydroxyethoxy group is extended away from the molecule. There are two stacks of 'dimers' of BHTCNQ molecules along [001]; these stacks, mutually related by the glide-plane operation, form a 'herringbone' pattern. The least-squares six-membered ring in the first stack is tilted by 56° to [001] (and tilted by 95° to the equivalent plane in the second stack), with interplanar distances of 3.500 and 3.831 Å

* Supported in part by the National Science Foundation, Grant DMR-84-17563.

† On leave at Department of Chemistry, University of Alabama, Tuscaloosa, AL 35487-0336, USA. Permanent address: Science Department, Laramie County Community College, Cheyenne, WY 82007-3299, USA.

‡ Present address: ARCO Research Center, Newtown Square, PA 19073, USA.

§ Present address: Department of Applied Chemistry, Faculty of Engineering, Osaka City University, Sugimoto-cho, Sumiyoshi-ku, Osaka, Japan.

¶ To whom correspondence should be addressed.